

Aspects of Fiber Morphology Affecting Properties of Handsheets Made from Loblolly Pine Refiner Groundwood

By CHARLES W. McMILLIN*, Alexandria, La.

Summary

In *Pinus taeda* L., burst, breaking length, and sheet density were improved by using fiber refined from wood having long, narrow-diameter tracheids with thick walls. Only narrow-diameter tracheids with thick walls were required to improve tear factor. A theoretical stress analysis revealed that thick-walled cells of small outside diameter fail by diagonal tension or parallel shear, depending on the fibril angle, while under torsional stress during refining. Such failures result in ribbon-like fragments which research elsewhere has demonstrated to provide the coherence necessary for strength development in mechanical pulps. In contrast, thinned cells of small outside diameter fail by diagonal compression and yield few ribbons. Long fibers are more desirable than short fibers because of greater induced stresses and improved chances of axial alignment between the disks.

Zusammenfassung

Berstdruck, Reißlänge und Blattichte von *Pinus taeda* L., wurden durch Verwendung von feiner Fasern aus Holz, das lange Tracheiden mit geringem Durchmesser und dicken Wänden besitzt, verbessert. Zur Verbesserung des Reißfaktors waren ausschließlich dickwandige Tracheiden mit geringem Durchmesser erforderlich. Eine Spannungsanalyse zeigte, daß dickwandige Zellen mit kleinem Außendurchmesser durch diagonale Zug- oder parallele Scherbeanspruchung in Abhängigkeit vom Fibrillenanstiegswinkel während der Torsionsbelastung an Refiner reißen. Durch diesen Bruchvorgang ergeben sich bandförmige Bruchstücke, die schgewiesenermaßen notwendig sind, um den inneren Zusammenhalt für die Festigkeitsentwicklung in mechanischem Zellstoff zu ermöglichen. Im Gegensatz hierzu brechen dünnwandige Zellen mit kleinem Außendurchmesser mehr durch diagonale Druckbeanspruchung, und es ergeben sich nur wenige Bänder. Lange Fasern sind insofern erwünschter als kurze, da sie zu höheren Festigkeiten führen und eine höhere Wahrscheinlichkeit ihrer axialen Ausrichtung zwischen den Refinerscheiben besteht.

Introduction

A program of research to establish the interrelations between pulp quality, chemical composition, wood morphology, gross wood properties, degree of fiber refining, and the properties of paper handsheets has been undertaken at Alexandria, Louisiana. The ultimate objective is to develop criteria useful in predicting and controlling the papermaking potential of refiner groundwood from loblolly pine (*Pinus taeda* L.).

A previous paper [McMILLIN 1968] examined the interrelationships between refining energy, gross wood characteristics, and the physical properties of handsheets. Burst, tear, and breaking length were shown to be increased by application of high refining energy and use of fast-grown wood that contains a high proportion of latewood but is of relatively low density. Only high refining energy and high proportion of latewood were required to improve sheet density. These results

* The author appreciatively acknowledges the assistance of the Roy O. Martin Lumber Co., Alexandria, La.; R. A. LEASK and J. ADAMS of Bauer Bros. Co., Springfield, Ohio; and J. BOWER, statistician at the Southern Forest Experiment Station, New Orleans, La.

suggest that sheet properties can be improved or made more uniform by selection of wood having the desired characteristics or by modification of refining procedures in accordance with wood quality.

Gross wood characteristics are relatively easy to measure and are therefore useful in identifying wood types. However, it is difficult to interpret these gross factors in terms of their causal relationships with sheet properties. For example, wood specific gravity is, in part, determined by the morphological characteristics of early- and latewood tracheids and the relative amounts of each tissue type. Hence, quantitative data in terms of fiber characteristics should prove more useful than specific gravity in guiding research in wood quality and in the paper technology of refiner groundwood.

This paper discusses the interrelationships between loblolly pine fiber characteristics and the physical properties of handsheets. Subsequent articles will consider pulp quality and chemical composition of wood in relation to handsheet strength.

Procedure

The detailed procedures for selection of trees, wood preparation and classification, refining, chip sampling, and handsheet testing have all been described previously [McMILLIN 1968] and are therefore only summarized here.

Wood was selected and stratified into 12 categories. Two growth rates (less than 6 rings per inch and more than 6 rings per inch), two specific gravities (less than 0.49 and more than 0.49), and three radial positions in the stem (0 ... 10, 11 ... 20, and 21 ... 30 rings from the pith) were considered in a factorial design. The wood in each category was chipped and the chips randomly divided into four within-sample replications. The 48 samples of chips were then fiberized in a double-disk refiner; consistency was 20 percent and refining energy was 40 hp days per air-dry ton on the first pass and 30 hp days on the second. Identical samples of wood stratified as above were refined in a single pass, but pulps were inferior to those obtained from double-pass fiber and therefore are not considered here.

Since the purpose of the study was to establish basic relationships, no attempt was made to optimize sheet properties, for example, by applying higher refining energies. Because of the factorial nature of the experimental design (all combinations of all selected levels of specific gravity, growth rate, radial position, and passes through refiner), and because of the widely divergent wood types, it was necessary to select refining energies that could achieve fiberization in all wood categories in both one and two passes. High refining energies were not possible with all wood types, i.e., with certain types high energy inputs would have resulted in zero plate clearance. Because of this necessary limitation, the double-pass pulps were of lower quality than would generally be attained in commercial practice.

Handsheets were formed by the TAPPI standard method. Four sheet properties were determined: sheet density, burst factor, tear factor, and breaking length.

A subsample of chips was drawn from each replication for determination of wood fiber characteristics. Four morphological properties were measured for both earlywood and latewood — single cell-wall thickness, radial lumen diameter, radial tracheid width, and tracheid length — and correlated with the four sheet properties. All morphological characteristics were determined on samples used in the earlier study.

Tracheid length was evaluated from 40 randomly selected chips. Chips were bisected into earlywood and latewood slivers and macerated in a 50/50 solution of 30 percent hydrogen peroxide and glacial acetic acid for 2 days at 50° C. Samples of the macerated material were mounted in water on 10 glass slides. With a calibrated projection microscope ($\times 40$), five tracheids were measured on each slide, the five unbroken tracheids lying adjacent to a dot on the center of the projection screen. Thus 50 observations were made on each subsample.

On different tracheids (macerated as described above) single cell-wall thickness, lumen diameter, and tracheid diameter for both earlywood and latewood were separately determined by viewing the radial fiber surface. Fifty observations of each dimension were made at the midpoint of the tracheid (5 observations on each of 10 slides) with a compound microscope equipped with a Filar eyepiece. Radial surfaces were identified by the presence of pits. Thickness of both cell walls was measured and the results averaged for each observation.

Processing the Data

To identify possible trends, individual handsheet properties were first plotted against the measured morphological characteristics. In most cases, no single relationship was apparent between a given sheet property and a single early- or latewood morphological characteristic. Multiple regression analysis of these data did not develop useful relations.

Since a paper handsheet is a composite of both earlywood and latewood fibers, a weighting system was employed to describe average composite morphological characteristics, e.g., average earlywood-latewood tracheid length. If the dimensions of cells in the tangential direction are assumed constant at unity, it can be shown that a given average morphological property for the earlywood and latewood composite is a function of the number of cells per unit volume of each tissue type and their respective volume percentages. From this analysis, the following weighting equation was developed.

$$P = \frac{(1 - LW) (P_e)}{(ET) (ETD)} + \frac{(LW) (P_l)}{(LT) (LTD)} + \frac{(LW)}{(LT) (LTD)}$$

where:

P = a weighted morphological characteristic of the earlywood-latewood composite, P_e = a morphological characteristic of earlywood, P_l = a morphological characteristic of latewood, W = proportion of latewood, ET = earlywood tracheid length (millimeters), ETD = earlywood tracheid diameter (micrometers), LT = latewood tracheid length (millimeters), LTD = latewood tracheid diameter (micrometers).

The fiber characteristics of Table 1 were derived by this weighting procedure. The proportion-of-latewood values used in the weighting equation were those obtained in the earlier study, as are the handsheet properties listed in Table 1.

The data in the table were used in multiple regression analyses. Equations were developed by stepwise introduction of the independent variables (48 observations) in order of their individual contribution to the cumulative R^2 . All equations were of the type: $y = b_0 + b_1x_1 + b_2x_2 + \dots$, where y is a dependent variable, e.g., burst, tear; b_i , a regression coefficient; and x_i , an independent

variable, e.g., weighted average tracheid length, weighted average cell-wall thickness. All equations were tested at the 95 percent level of probability, and all variables were significant at that level.

Various combinations and transformations of the single variables were included in the analysis.

The single variables were:

TL = weighted average tracheid length (millimeters), CWT = weighted average cell-wall thickness (micrometers), LD = weighted average lumen diameter (micrometers), TD = weighted average tracheid diameter (micrometers).

The combinations and transformations were:

$$\begin{aligned} & (LD)/(TD) \\ & 1/(TD) \\ & (TL)/(TD) \\ & (TD)/(TD - LD) \\ & (TL)^2 \\ & (LD)^2 \\ & (CWT)^2 \\ & (TD)^2 \\ & [(TD)^2 - (LD)^2] (TL) \\ & (TL) (CWT)/(TD) \\ & 2(CWT)/(LD) \end{aligned}$$

Results

Several of the morphological characteristics listed in Table 1 were correlated. For the 48 observations, cell-wall thickness¹ was positively correlated with tracheid length ($r = 0.591$) and negatively correlated with lumen diameter ($r = -0.698$) and tracheid diameter ($r = -0.434$). Lumen diameter was highly correlated with tracheid diameter ($r = 0.945$). All other correlations were low.

As in the earlier study, sheet properties also proved interrelated. Sheet density was positively correlated with burst factor ($r = 0.616$), tear factor ($r = 0.526$), and breaking length ($r = 0.629$). Burst factor was positively correlated with breaking length ($r = 0.962$) and tear factor ($r = 0.934$), while tear factor was positively correlated with breaking length ($r = 0.929$). Variance analysis showed no significant difference in refining energy between pulps.

Table 2 lists multiple regression equations which most accurately describe handsheet properties in terms of weighted average morphological characteristics.

Sheet Density

The best equation for sheet density (Eq. (1)) accounted for 17 percent of the total variation, with a standard error of 0.02. Sheet density was significantly related to the product of tracheid length and cell-wall thickness divided by tracheid diameter.

Fig. 1 shows the effect of these variables on sheet density. This figure and Figs. 2 through 4 were obtained by substituting a range of values of the variables on the X-axis and fixing the remaining variables at the indicated levels. Lumen diameter varied with tracheid diameter by the lineal regression equation:

$$LD = -23.4844 + 1.2239 (TD) \quad (R^2 = 0.893) .$$

¹ All morphological characteristics discussed subsequently are weighted averages.

he relations plotted consider only the range of variation contained within the range of all variables.

From Eq. (1) and Fig. 1, sheet density increased with increasing tracheid length for all sampled levels of tracheid diameter and wall thickness. The level and slope

Table 1. *Weighted Wood Characteristics and Handsheet Properties*¹

Position in tree (rings from pith)	Unextracted specific gravity	Rings per inch	Cell wall thickness ² μm	Lumen diameter ² μm	Tracheid width ² μm
0—10	0.427	4.11	5.4	38.2	49.0
0—10	.457	7.59	6.2	38.1	50.1
0—10	.492	4.80	6.1	32.5	44.7
0—10	.515	11.83	6.2	30.1	42.6
11—20	.445	5.53	6.7	34.1	47.5
11—20	.459	7.08	6.7	34.9	48.0
11—20	.512	5.30	7.3	28.6	43.0
11—20	.524	12.38	7.1	28.3	42.5
21—30	.458	4.91	6.6	33.2	46.6
21—30	.438	8.27	7.0	32.9	46.6
21—30	.534	5.53	7.2	29.7	43.8
21—30	.511	8.27	7.7	29.3	44.6

Position in tree (rings from pith)	Tracheid length mm	Sheet density g/cm ³	Burst factor	Tear factor	Breaking length
0—10	3.53	0.289	3.34	41.7	604.3
0—10	3.71	.281	3.25	42.2	720.5
0—10	3.34	.266	3.82	48.9	761.0
0—10	3.64	.293	2.96	35.5	656.1
11—20	3.85	.287	4.41	54.3	896.1
11—20	4.11	.293	4.87	58.4	996.1
11—20	3.73	.318	6.42	82.2	1,264.0
11—20	3.73	.292	3.23	41.3	724.2
21—30	4.07	.291	5.61	67.0	1,096.9
21—30	4.18	.319	7.00	76.5	1,312.4
21—30	3.92	.302	5.49	61.3	1,085.3
21—30	4.16	.299	5.67	61.7	1,129.3

¹ Each numerical value is the average of four replications.

² μm = micrometer = 10⁻³ millimeters = 10⁻⁶ meters.

the sheet density-tracheid length relationship increased with increasing cell-wall thickness but decreased with increasing tracheid diameter. Although not shown here, the effect of a variable in the denominator of a regression equation is generally curvilinear.

Table 2. *Multiple Regression Equations Developed to Estimate Sheet Properties*

Property	Equation	Variable	Coefficient	Cumulative R^2	Standard error of estimate
Sheet density	1		b_0 0.2451		
		(TL) (CWT)	b_1 0.7350	0.169	0.02
Burst factor	2	(TD)	b_0 -0.8456		
		(TL) (CWT)	b_1 15.8218	0.373	
Tear factor	3	$\frac{2(\text{CWT})}{(\text{LD})}$	b_2 -7.1993	0.477	1.02
		$\frac{2(\text{CWT})}{(\text{LD})}$	b_0 792.2751		
		$\frac{(\text{LD})}{(\text{TD})}$	b_1 -274.6336	0.378	
		$\frac{(\text{LD})}{(\text{TD})}$	b_2 -1,151.4235	0.434	
		$\frac{(\text{TD})}{(\text{TD} - \text{LD})}$	b_3 34.3296	0.518	
Breaking length	4	$\frac{(\text{CWT})^2}{(\text{CWT})^2}$	b_4 1.3646	0.563	10.16
		(TL) (CWT)	b_0 13,285.3726		
		(TD)	b_1 3,660.5067	0.453	
		$\frac{2(\text{CWT})}{(\text{LD})}$	b_2 -4,602.1215	0.556	
		$\frac{(\text{LD})}{(\text{TD})}$	b_3 -18,318.4190	0.597	
		$\frac{(\text{LD})}{(\text{TD})}$	b_4 537.5837	0.691	
		$\frac{(\text{TD} - \text{LD})}{(\text{TD})}$	b_5 -19,569.7859	0.740	133.20

For all significant variables within the range of data, sheet density was increased by using fiber refined from wood having long tracheids with narrow diameters and thick cell walls.

Burst Factor

The best multiple regression equation for burst factor accounted for 48 percent of the total variation with a standard error of 1.03. Burst was a complex function of tracheid length, cell-wall thickness, tracheid diameter, and lumen diameter.

As shown in Fig. 2, burst increased with increasing tracheid length for all levels of cell-wall thickness and tracheid diameter. The level and the slope of the relationship of burst to tracheid length increased with increasing cell-wall thickness and decreased with increasing tracheid diameter.

All significant variables considered, burst strength was greatest in sheets made from fiber refined from wood having long tracheids with narrow diameters and thick cell walls.

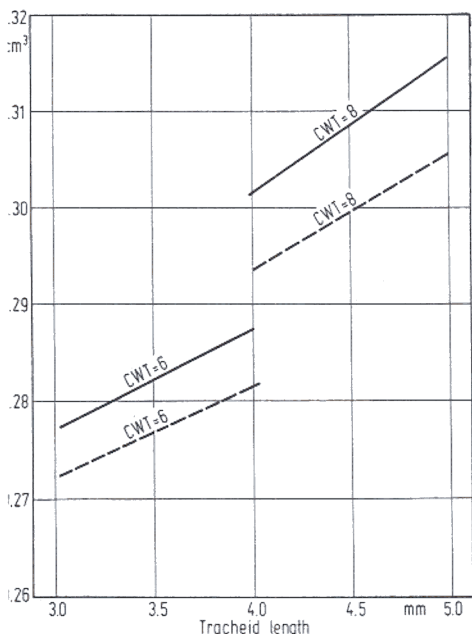


Fig. 1. Effect of tracheid length, cell-wall thickness (in micrometers), and tracheid diameter on sheet density. The dotted lines in this figure and in Figs. 2 through 4 plot tracheids having outside diameters of 49 micrometers. The solid lines plot tracheids having outside diameters of 42 micrometers.

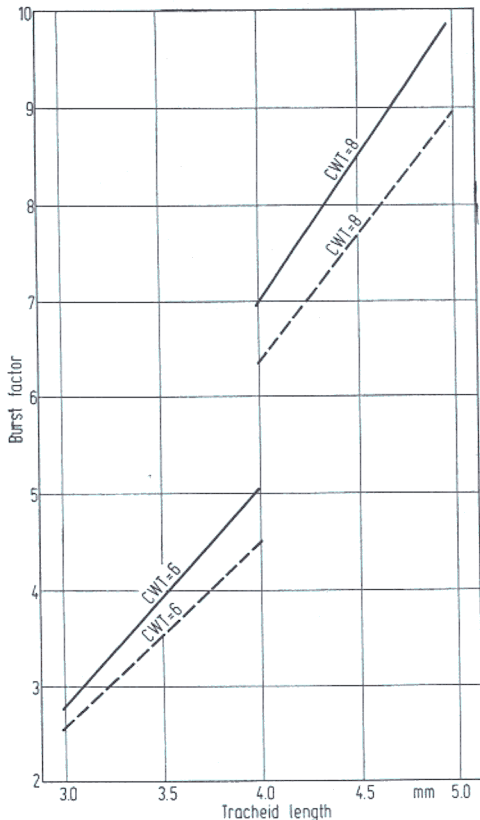


Fig. 2. Effect of tracheid length, cell-wall thickness, and tracheid diameter on burst factor.

Tear Factor

Eq. (3) accounted for 56 percent of the variation in tear strength. The standard error of the estimate was 10.1. Tear factor was a complex function of lumen diameter, tracheid diameter, and cell-wall thickness. Tracheid length did not prove significant.

From Eq. (3) and Fig. 3, tear factor increased in a curvilinear manner with increasing cell-wall thickness for tracheids of large diameter, while it decreased slightly with increasing wall thickness for tracheids of small diameter. For a given wall thickness, tear factor increased with decreasing tracheid diameter.

All factors considered, tear factor was increased by using fiber refined from wood having narrow tracheids with thick walls.

Breaking Length

This property was related to a function of tracheid length, lumen diameter, tracheid diameter, and cell-wall thickness. Eq. (4) accounted for 74 percent of the variation, with a standard error of 133.2.

As shown in Fig. 4, breaking length increased with increasing tracheid length for all sampled levels of tracheid diameter and cell-wall thickness. Both the level and the slope of the breaking-length/tracheid-length relationship increased with

increasing cell-wall thickness. Only the level increased with decreasing tracheid diameter.

All variables considered, breaking length was increased by using fiber refined from wood having long, narrow tracheids with thick walls.

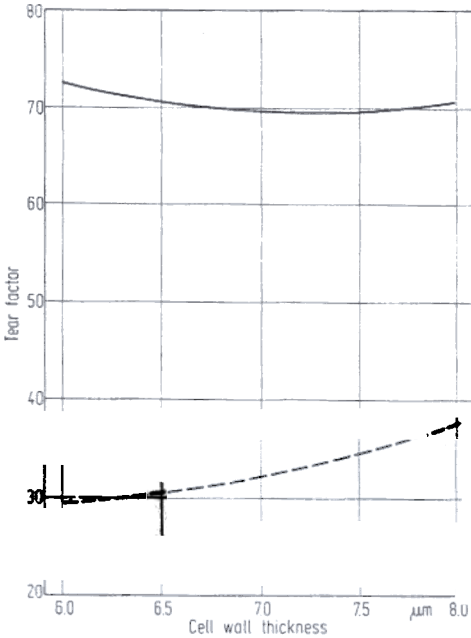


Fig. 3. Effect of cell-wall thickness and tracheid diameter on tear factor.

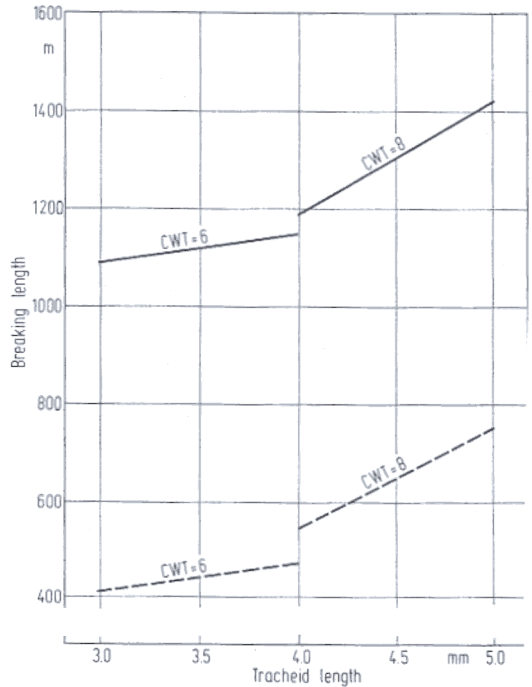


Fig. 4. Effect of tracheid length, cell-wall thickness, and tracheid diameter on breaking length.

Discussion

ATAK and MAY [1963] have described three phases of mechanical breakdown during the reduction of chips to fiber by double-disk refining. The first phase, occurring in the breaker-bar section, produces slender, matchstick fragments whose major axes lie in the direction of the wood grain. In a second phase these fragments are processed into partially or completely separated fibers. Lastly, the fibers are refined into papermaking pulp. During this final phase, additional refining may occur on the disk periphery by visco-elastic deformation of cylindrical fiber clumps [MAY, MORRIS, ATAK 1963].

FORGACS [1963] has demonstrated that coherence and strength development in paper from groundwood are principally provided by ribbon-like, fibrillar particles consisting mainly of the S_2 layer of the cell wall. Since such particles are highly flexible and deformable, they are brought into close contact with neighboring particles by the surface tension forces acting on them during drying. Thus, conditions favorable to hydrogen bonding are created. These ribbon-like particles were shown to be derived from the parent tracheids by unravelling of the S_2 layer after propagation of cracks in the direction of the S_2 helix.

FORGACS contends that unravelling results from rolling of intact isolated fibers or fiber bundles between the refiner plates. With chunks or fragmented parts of tracheids, the chance of unravelling is reduced since the available lengths of the layer in the direction of the helix may be too small to promote propagation of splits.

Microscopic examination of the pulps used in the present study, and strength determinations of handsheets made from them, confirm the observations of FORGACS. Pulps containing well-separated fibers with a high proportion of ribbons and fibrils characteristically resulted in stronger handsheets than those from pulps containing poorly separated fibers and chunks and low proportions of ribbons.

It seems possible that ribbons are formed through an interaction between forces developed within an intact fiber during refining and the morphological characteristics of the fiber.

Although an exact theoretical stress analysis is confounded by thermo- and hydrodynamic effects and the anisotropic nature of fibers, an approximate solution can be developed that is in reasonable agreement with the observed morphological characteristics and handsheet strength.

Consider a uniform, smooth-sided, right-cylindrical, intact fiber consisting only of the S_2 layer and having outside diameter d_o , inside diameter d_i , and length L . Assume that during the latter phases of refining the fiber becomes radially aligned between the surfaces of two counter-rotating disks of radius R revolving at speed S (Fig. 5A). If there is no slippage, the fiber tends to rotate about its longitudinal axis $X-X'$ at a velocity proportional to the rotational velocity of the disk at distance R' from disk center. Because the velocity of the disk varies directly with the disk radius, the rotational velocity at point B' on the fiber is greater than the velocity at point B , i.e., the radius of the disk is slightly greater at point B' than at point B . Since the fiber tends to rotate a greater distance per unit time at point B' than at point B , it is acted upon by a couple of equal numerical moment but opposite sign. Under these conditions, the fiber may be analyzed as a hollow circular shaft stressed in torsion.

If the undeformed fiber is considered to be held in mechanical equilibrium, Fig. 5B approximates the force relationships existing within it. Under torsion, the shaft is twisted by a couple $P-P'$. The magnitude of the couple will be a function of the difference between the rotational velocities at distance L apart. Elements of the surface become helices of angle α , and a radius is rotated through an angle β in length L . The state of stress of an element from the surface is pure shear (Fig. 5C). Pure tension of the same magnitude as the shear stress is produced across the plane $A-A'$ at an angle of 45° with the direction of the shear stress. There is an equal compressive stress on a plane $B-B'$ at right angles to the tension plane. The stress in shear on the outer surface of a hollow, circular cylinder in torsion is given by

$$S_s = \frac{16(T)(d_o)}{\pi(d_o^4 - d_i^4)}$$

where:

S_s = stress in shear, T = torsional moment, d_o = outside diameter, d_i = inside diameter.

As previously noted, ribbons are produced when the S_2 layer of the tracheid wall is first cracked parallel to the fibril helix (angle F , Fig. 5C) and then unwound.

It is generally held that the cell-wall microfibrils adhere strongly in large aggregates — termed fibrils — and that a zone of weakness exists between these aggregates. To produce the desired crack, the cell wall must be stressed in excess of the tensile or shear strength of the zone of weakness.

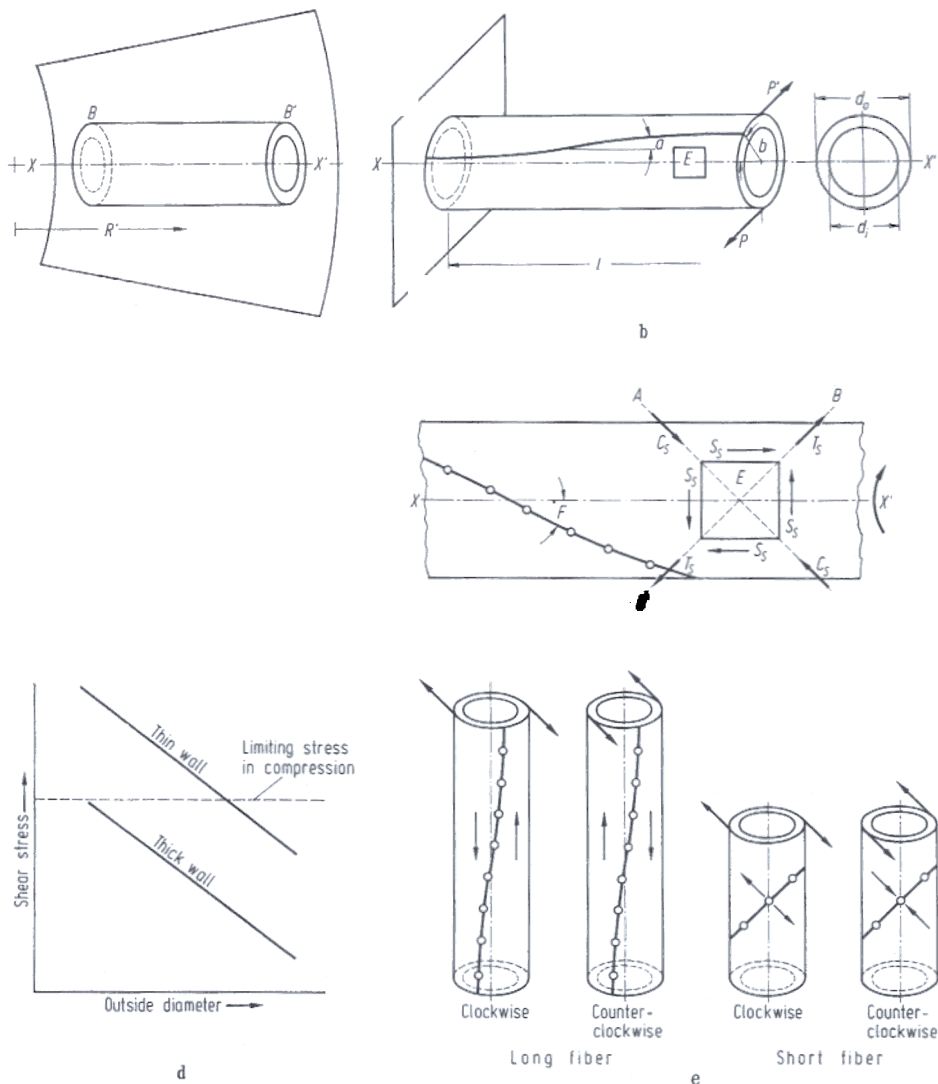


Fig. 5. Force relationships within an intact fiber during refining

For a given torsional moment, shearing stresses S_s of equal magnitude are introduced parallel and perpendicular to the axis of the particle. They are accompanied by diagonal tensile (T_s) and compressive (C_s) stresses of equal magnitude.

Since the fiber is a nonbrittle, visco-elastic material, failure in shear perpendicular to the rotational axis is unlikely. The equation and Fig. 5D show that a cy-

ider with small outside diameter develops greater stress than a large-diameter linder when subjected to a given torsional moment. For a given outside diameter, stress is greater in thin-walled than in thick-walled shafts. If the stress level exceeds the strength in compression (dotted line in Fig. 5D) before the strengths in parallel shear or diagonal tension are exceeded, failure is likely to occur by diagonal buckling. Thus, failure by diagonal buckling typically occurs in thin-walled, large-diameter fibers. As a result, cracks do not form, and the fiber is unable to unwind into the desired ribbon.

If the strength in shear parallel to the fiber axis or in diagonal tension is exceeded before the strength in diagonal compression, cracks can form parallel to the fibril helix and permit subsequent unwinding through visco-elastic deformations or pure rolling. Thick-walled fibers of small outside diameter favor this failure mechanism, since the stress level tends not to exceed the strength in diagonal compression.

If, for a fiber of given diameter and wall thickness, the zone of weakness delineated by the fibril helix is nearly parallel to the parallel shearing stress (angle F in Fig. 5C is small), the strength in shear parallel to the fiber axis may be exceeded. Long fibers, because of their relatively small fibril angle, are prone to this failure type if the torque is applied in either clockwise or counterclockwise direction (Fig. 5E). Shorter fibers with characteristically larger fibril angles tend to fail by diagonal tension when the torque is applied in a clockwise direction. With such fibers, the strength in tension would be exceeded before the parallel shearing strength. A short fiber twisted counterclockwise would tend to buckle, since the rear plane is not highly stressed and the plane of weakness is stressed in compression. Conditions are more favorable for ribbon formation with a long fiber than with a short fiber because of higher stresses resulting from the greater differential rotational velocity between the two ends. Furthermore, long fibers have better chances of attaining a true axial alignment than do short fibers. Clockwise rotation of the fibers appears desirable since the induced stresses are in a favorable direction with respect to the zone of weakness over a greater range of fiber lengths.

This analysis of torsional stresses applied to a cylindrical fiber during processing agrees with the experimental results in terms of optimum tracheid dimensions for improving properties of handsheets.

References

- ACK, D., and W. D. MAY: Mechanical reduction of chips by double-disk refining. *Pulp Pap. Mag. Can.* **64** (1963) No. C, T75/T83, T118.
- BERGACS, O. L.: The characterization of mechanical pulp. *Pulp Pap. Mag. Can.* **64** (1963) No. C, T89/T118.
- MAY, W. D., E. L. MORRIS and D. ATTACK: Dynamics of a visco-elastic wear particle between sliding surfaces. *J. Appl. Phys.* **34** (1963) 1920/1928.
- MILLIN, C. W.: Gross wood characteristics affecting properties of handsheets made from Loblolly pine refiner groundwood. *TAPPI* **51** (1968) 51/56.

(Received November 6, 1968)

CHARLES W. McMILLIN, Wood Scientist, Southern Forest Experiment Station,
USDA Forest Service, Alexandria, Louisiana.